Evaluation of fiber orientation in a composite and its effect on material behavior

Tatiana Mishurova[1], Fabien Léonard[1], Tyler Oesch[1], Dietmar Meinel[1], Giovanni Bruno[1], Natalia Rachmatulin[1], Patrick Fontana[1], Igor Sevostianov[2]

[1] Bundesanstalt für Materialforschung und –prüfung (Federal Institute for Materials Research and Testing), Unter den Eichen 87, 12205 Berlin, Germany. e-mail: tatiana.mishurova@bam.de

[2] Department of Mechanical and Aerospace Engineering, New Mexico State University, Las Cruces, NM 88001, USA.

Abstract

The reinforcement of concrete with polymer fibers provides resistance to crack formation. The orientation distribution of these fibers has a significant influence on the mechanical behavior of the material. To optimize material performance, micromechanical models that are capable of making accurate predictions of the mechanical behavior of composite materials are needed. These models must be calibrated using experimental results from microstructural characterization. For the fiber orientation distribution analysis in the present study, computed tomography (CT) data were used to evaluate the properties of a fiber-reinforced cement mortar. The results have indicated that the fibers in this material have highly anisotropic orientation characteristics and that there is a clear tendency for the polymer fibers to agglomerate during mixing and casting. The incorporation of this experimental data into micromechanical models will increase the accuracy of those models for material simulation and optimization.

Keywords: Orientation Distribution, Fiber-Reinforced Concrete, Computed Tomography.

1. Introduction

1.1. History and Potential of Fiber-Reinforced Concretes

The use of fiber-reinforced cement materials has a long history dating back to at least 1900 with the introduction of asbestos cement [1]. These early fiber-reinforced cement materials were primarily used for the manufacture of panels to be employed as roofing and cladding. The utilization of fibers in concrete materials for building construction only began during the 1970s [2].

The main disadvantage of all cementitious materials is their low tensile strength. Tensile stresses might develop as a result of mechanical loading or constrained deformation caused by changes in moisture content or in temperature. Such deformations may occur already a few hours after placing the material, and lead to damage in the form of cracking when the tensile stresses exceed the initially low tensile strength. In conventional reinforced concrete, substantial elongation is needed for steel reinforcing bars to carry significant tensile forces across cracks. If these cracks are wide, they can lead to durability problems through both freeze-thaw cracking and through the movement of chlorides causing corrosion to the steel reinforcing bars. The size and spacing of reinforcing steel is a dominant factor in determining the size of cracks [3].

Fiber-reinforced concrete (FRC) may be viewed as reinforced concrete with extremely small and closely-spaced reinforcing bars. Polymer fibers can even be used in FRC as a replacement for conventional steel reinforcement. The use of FRC in structural members, such as in beams and columns, has shown that great ductility can be achieved with cracks that are barely visible to the naked eye, limiting both corrosion and freeze-thaw damage [4]. Polymer fibers can also mitigate plastic shrinkage cracking [5], prevent explosive spalling in the case of dense high-performance concrete during fire attack [6], and, even with low elastic modulus, considerably improve the strain capacity, the toughness and impact resistance of FRC composites [7]. Fibers have also been utilized in many recent high-performance concretes to achieve very high tensile strengths [8-10]. These characteristics of FRC have the potential to allow for the construction of lighter, more sustainable, and more energy efficient structures.

At the present time the promise of FRC has not been fully realized because of challenges that remain with its implementation and characterization. Previous research has demonstrated that the performance of FRC members is highly dependent on internal fiber orientations and distributions [7, 11-15]. These fiber orientations are often highly anisotropic in nature and are the result of material flow patterns during the casting process [13, 16-17]. Polymer fibers in concrete are also difficult to distribute with defined orientation during material production due to the tendency of the fibers to agglomerate. This agglomeration can negatively affect the workability and the mechanical performance of the material. Characterizing the effect of parameters like volume fraction, fiber dimensions and special fiber surface treatments on the orientation distribution of fibers is important for estimating mechanical properties of the material and accurately modeling its behavior. These anisotropic characteristics of FRC have major safety implications for its widespread use since material anisotropy can lead to planes of weakness within structural members. When not properly controlled, these weak planes can become aligned with the primary plane of stress and cause premature failure.

1.2. Use of CT for Analysis of Concretes and FRCs

To collect information about fiber orientation distribution in a material, either non-destructive testing (inductivity-based assessment, resistivity-based assessment, etc.) or destructive testing (metallography, microscopy, etc.) methods can be used [18]. However, only X-ray computed tomography (CT) provides 3D information about fiber distribution without difficult sample preparation as it requires only a difference in the linear X-ray attenuation coefficients of the matrix and reinforcement, disregarding other physical properties.

X-ray CT has been applied to concrete research problems for over 30 years. Initially, CT was primarily used for the simple identification of internal objects within concrete specimens [19, 20]. Since then, CT-based techniques have been applied to a number of additional concrete materials problems, including investigating the nature of concrete pore structure and studying sulfate attack [21-23]. Recently, these CT-based analysis methods have been enhanced for the evaluation of more complex material behavior phenomena such as the quantitative measurement of concrete fracture and damage parameters [17, 24, 25].

Quantitative analysis of CT images can also provide important information about the spatial distribution and directional orientation of individual material components within a given sample [24, 26-27]. For concrete, these components can include aggregate, mortar, fibers, and voids. Such techniques are particularly useful for studying the causes of fiber anisotropy within FRC and how that anisotropy affects cracking patterns. Algorithms can also be tailored to evaluate the nature of damage to the fibers and predict the relative amount of energy expended by different fiber failure mechanisms [28].

1.3. Potential and Significance of Modeling

In fiber reinforced composites, the fibers are usually neither perfectly parallel, nor perfectly randomly oriented, but have a certain orientation distribution, which is one of the major factors affecting the material behavior [29]. At the present time, the most popular theoretical scheme for the calculation of fiber orientation distributions is the so-called orientation distribution function (ODF) [30]. However, critical to the optimization and implementation of FRCs is the experimental evaluation of the ODF and its incorporation into an analytical formula which can be used for micromechanical modeling [31].

Such models are currently in great need for the optimization of mix designs for high-performance concretes because they can predict mechanical properties of materials. There are a vast number of potential concrete components, such as fiber and aggregate types, commercially available as well as a variety of possible casting techniques. In order to identify optimized high-performance concrete mix designs and casting methods experimentally, a prohibitively large number of samples would have to be cast and tested. Using models incorporated with real fiber distribution information, however, it should be possible to digitally evaluate many thousands of possible material configurations. The most promising of these can then be validated through actual testing programs.

2. Experiments

For the CT measurements, cylindrical specimens with a length of 40 mm and a diameter of 10 mm (Figure 1) were cored from a cement-mortar prism with size 40 x 40 x 160 mm. Before drilling, the prism was dried with temperature of 40 °C and impregnated with epoxy resin in order to prevent disintegration of the sample. The matrix material consisted of Portland cement (CEM I 32.5 R), ground limestone, silica sand and polyacrylonitrile (PAN) fibers. The volume fraction of cement and limestone/sand in mixture was 30% and 70%, respectively. The fibers had a diameter of 15 µm and a length of 4 mm. The volume fraction of fibers in the material was 0.5%. The mortar prism was produced with a conventional mortar mixer in accordance with DIN EN 196-1 [32]. After mixing, test specimens were compacted by using a vibrating table and placed into a container with water for 24 hours. Then, all specimens were stored under water for 6 days with temperature of 20°C.

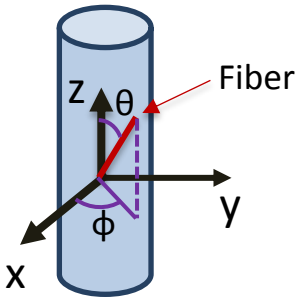

Figure 1: Schematic representation of sample with coordinate system used for fiber orientation analysis.

The CT measurements were performed by using a v|tome|x L 300 CT scanner from General Electric. During each scan, 3000 projections were acquired, with each projection acquired at a 0.12° rotation increment. A tube voltage of 80 keV and a tube current of 50µA were used during the scans and the acquisition time for each projection lasted 2 seconds. To obtain a better statistical sampling of the orientation distribution of fibers within each FRC sample, six CT measurements at different locations along the height of the sample were carried out, each with a spatial resolution of 6.65 µm.

3. Results

Figure 2 shows 2D reconstructed slices for two planes obtained from a 3D reconstruction. The polymer fibers are characterized by lower gray scale values in comparison with the matrix due to their lower X-ray attenuation level. Of particular note was the presence of several fiber agglomerations within the 3D sample volume (Figure 2b).

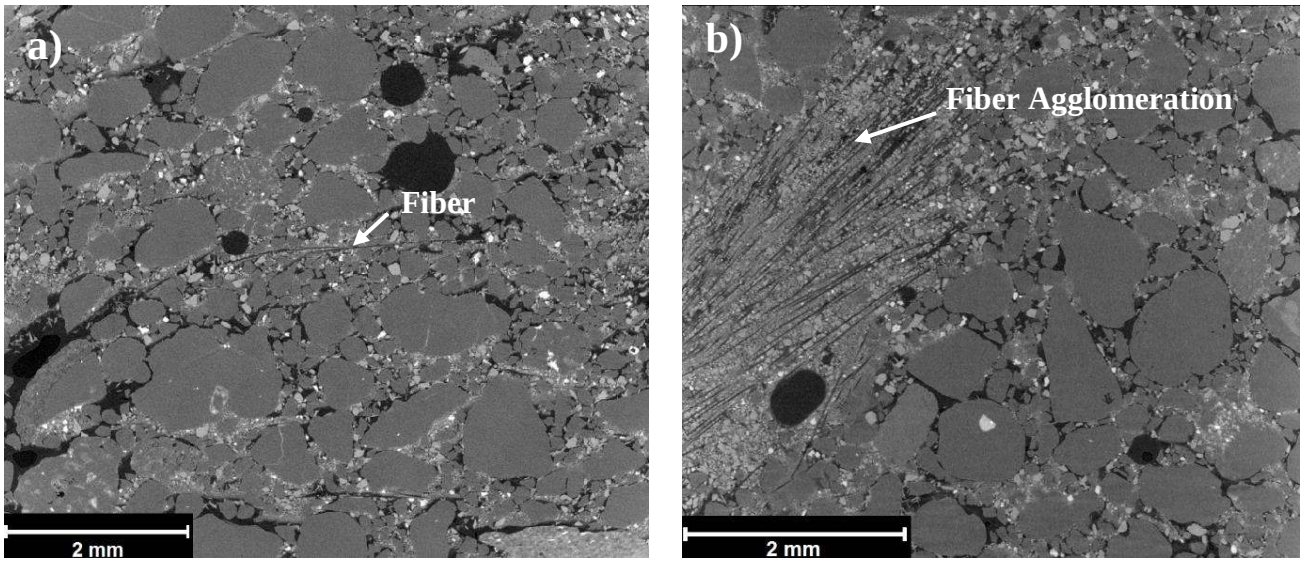

Figure 2: 2D reconstructed slices (a) in plane XY and (b) in plane XZ.

Image analysis of the reconstructed volumes was performed using the program Amira ZIB Edition from the Konrad-Zuse-Zentrum Berlin (ZIB) [33]. Due to the low difference in contrast between the fibers and matrix material, as well as the small diameter of the fibers (15 µm), identification of fibers by intensity segmentation was not possible. However, it was possible to trace fibers by using the template matching algorithm (cylinder correlation) implemented in Amira ZIB Edition. This tool calculates fiber distribution and orientation properties by comparing the reconstructed volume with a tube-like fiber template defined by the user. This approach helps to trace fibers even in noisy data. The parameters that were used for the template matching algorithm are presented in Table 1.

Parameter	Value, µm
Cylinder length	480
Mask cylinder radius	11.5
Outer cylinder radius	10.5
Inner cylinder radius	0
Contrast	Dark on Bright
Min Line Length	900

Table 1: Parameters used in the template matching algorithm.

When longer cylinder lengths were used for the analysis, it was found that the algorithm was less sensitive in properly identifying the ends of the fibers. The use of shorter cylinder lengths, however, also led to significantly longer computation times. Through a series of iterations during this analysis, a cylinder length of 480 µm was found to provide an optimal balance between fiber detection sensitivity and computation time. Increasing of mask cylinder radius was also found to decrease the sensitivity of the algorithm for identifying fibers in the agglomeration regions. Conversely, low mask cylinder radii were found to produce unsatisfactory results because they caused the template matching algorithm to misidentify aggregate borders as fibers. After a series of analysis iterations, the optimal balance in sensitivity and accuracy was obtained with a mask cylinder radius and an outer radius of 11.5 µm and 10.5 µm, respectively. The inner cylinder radius used during the analysis was, of course, 0 µm since the fibers did not contain hollow cores. In spite of this cylinder radius optimization, it is still probable that fibers in agglomeration

regions were detected less successfully than those in non-agglomeration regions and that their contribution to the fiber orientation analysis is, therefore, somewhat underestimated.

In the present study, the implementation of the template matching algorithm had some limitations. The crossing of low-density fibers with pores and aggregate, as well as the cutting of some fibers during sample extraction resulted in difficulties in estimating fiber length. Observations indicated that the bending of the fibers was not significant in this material. Therefore, reliable fiber orientation information could be extracted even from partial fibers. In regions with high concentrations of fibers (agglomeration) it was not possible to identify each individual fiber due to the limited spacing between fibers. The improper identification of material interface zones (such as the surface of aggregate particles) as fibers was be minimized by implementing additional software parameters such as length and bending control.

Two orientation angles (φ, θ) in a spherical coordinate system were obtained for each fiber from the Amira fiber-tracking algorithm. This reference coordinate system is shown in the Figure 1. The orientation distribution was obtained for six CT scans along sample height. However, a small, prismatic section of the sample (7 mm × 7 mm × 6 mm) was selected for representation of fiber orientation in Figure 3. Assuming symmetry within the spherical coordinate system, the orientation angle φ was calculated for half of the sphere (from 0° to 180°) and the orientation angle θ was calculated for one quarter of the sphere (from 0° to 90°). It was then possible to produce surface plots of fibers colored according to their orientation angles. Figure 3 shows a depiction of fiber orientations within the prismatic analysis volume for ordination angles φ (Figure 3a) and θ (Figure 3b). It is important to note that although fiber diameter was taken into account as part of the fiber identification algorithm, this algorithm only produced a series of centerline traces for the fibers. Thus, although these results are useful for identifying fiber location and orientation characteristics, they do not directly provide volume-related fiber information (such as fiber volume, diameter variation among fibers, etc.)

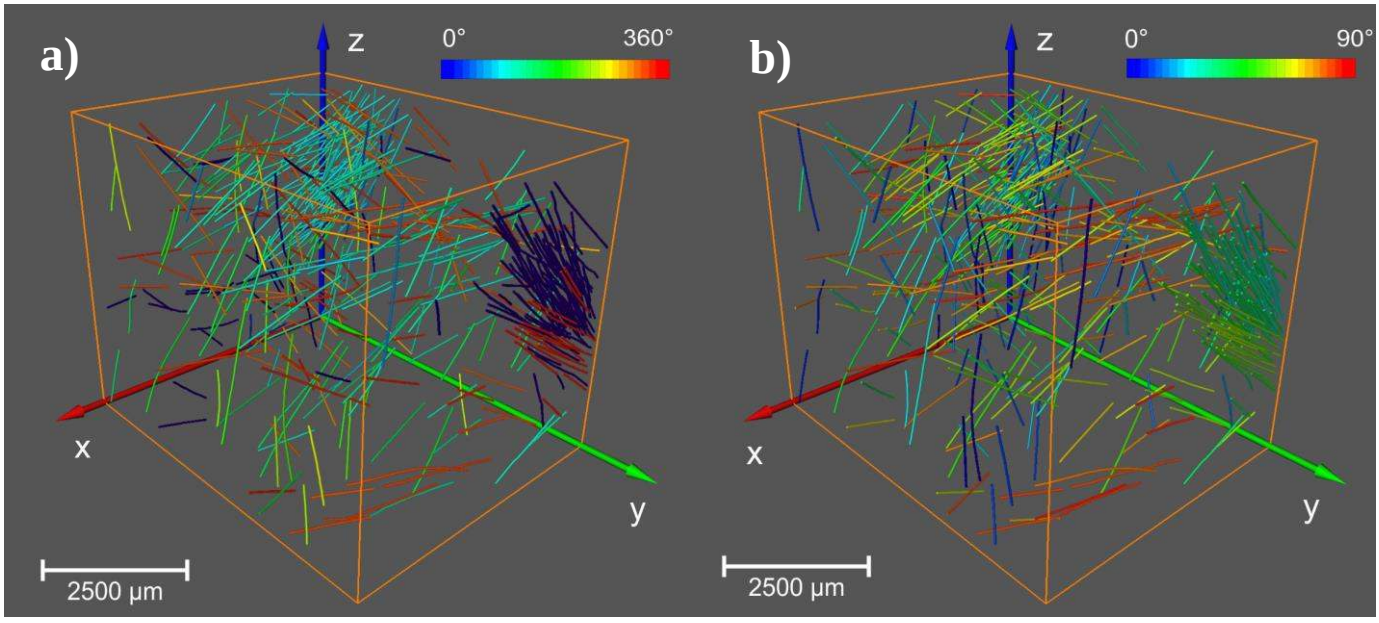

Figure 3: Depiction of fiber orientation distribution with respect to angle φ (a) and angle θ (b).

With subsequent data processing, these values were used to produce orientation distribution histograms (Figure 4). The results were normalized using the total number of fibers identified within all six CT scans of the analyzed sample (1278 fibers). From the orientation distribution histograms, it is clear that a disproportionate number of fibers was oriented roughly parallel to the X-Z plane (φ near 0° or 180°) (Figure 4a) and with an orientation angle θ larger than 45° (Figure 4b). As shown in Figures 2 and 3, in some regions of the sample agglomerations of fibers with similar orientation distribution were observed. These agglomerations indicate that the overall distribution of fibers was significantly inhomogeneous and the effect of these agglomerations can be recognized as the peaks in the fiber orientation distribution histograms.

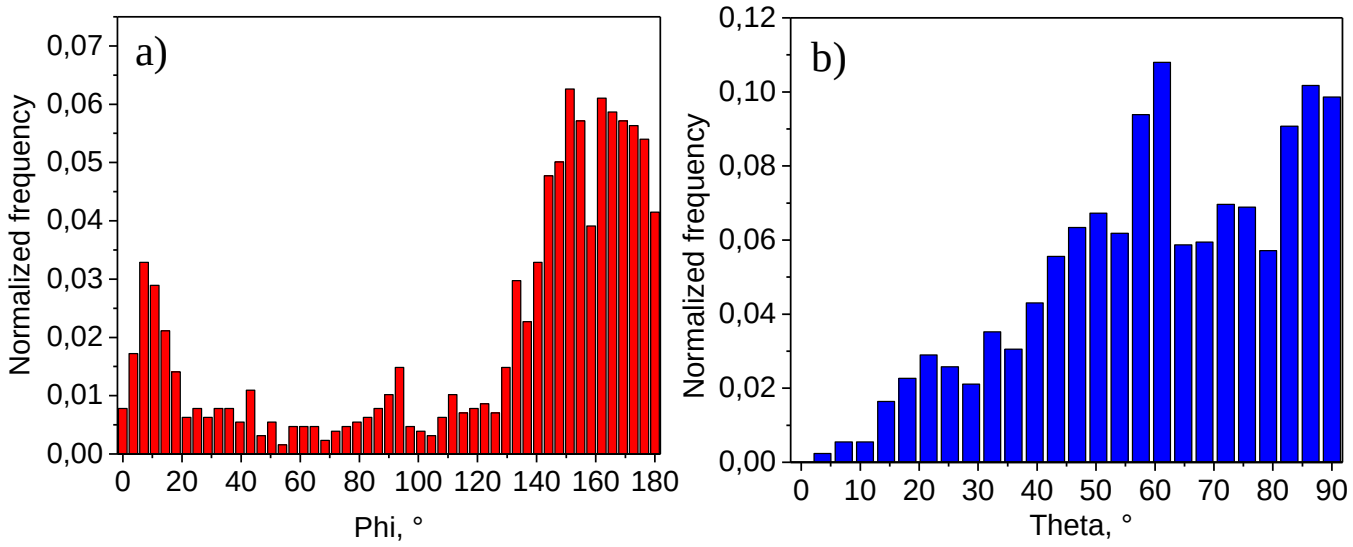

Figure 4: Orientation distribution histograms for angle φ (a) and angle θ (b).

The agglomeration of fibers indicates that there is a need for changing the mixing procedure. Different water/cement ratios cement should also be tested as well as changes in the volume fraction of fibers. In the present study, the PAN fibers had a hydrophobic surface which could have also contributed to the clustering of fibers during their contact with water. Therefore, the production and testing of fibers with a hydrophilic surface treatment is also proposed.

These fiber orientation distributions were then used as an experimental input for modeling the mechanical properties of the material. The resulting models were able to account for the anisotropic fiber orientation distributions through the use of a scatter parameter determined by non-linear least squared fitting of the histograms. Mechanical testing for validation of these models is also underway. A forthcoming publication will provide detailed information about the composition of these mechanical models and their success at predicting experimental material behavior.

Conclusion

Polymer fibers with small diameter were successfully detected within a concrete specimen through the use of CT and specialized image processing software. These results have indicated that there is a clear tendency of polymer fibers to agglomerate during mixing and casting. Future research is planned that will focus on the development of new fiber coatings and concrete casting techniques to minimize the inhomogeneity in fiber distribution.

Subsequent analysis of the fiber data also indicated that the orientation characteristics of the fibers were highly anisotropic in nature. These results suggest that planes of weakness will occur parallel to the primary orientation angle of the fibers. Such planes of weakness are due to the weak bond between mortar and polymer material and could lead to premature failure of structural components. Future research is also planned which will focus on eliminating this weakness through either achieving more uniform fiber orientation distributions or by controlling the anisotropic orientation plane of fibers to minimize the levels of stress along planes of weakness.

The fiber orientation distribution data of the FRC was then used as experimental input for micromechanical models. A forthcoming publication is planned which will detail the characteristics of these models and their validation through comparison with mechanical testing data. Such models are currently in great need for the optimization of mix designs for high-performance concretes. Through calibration and validation of these models, their accuracy can be improved with the goal of precisely predicting the effect that changes in concrete component materials and casting methods have on the overall mechanical properties of the material.

Acknowledgements

This work was supported by National Group of Mathematical Physics GNFM-IndAM (Italy), FP7 Project TAMER IRSES-GA-2013-610547, NASA Cooperative Agreement NNX15AL51H (through NM Space Grant Consortium), Bundesministerium für Bildung und Forschung (BMBF) grant 13N13306, and the BAM Visiting Scientist Grant Program. The authors are also grateful to Mr. Philipp Drabetzki (BAM, Berlin) for sample preparation.

References

[1] Eternit-Werke Ludwig Hatschek AG. "History," 2015, <http://www.eternit.at/9935.0.html>

[2] MatSE (Department of Materials Science and Engineering). "The History of Concrete: A Timeline," University of Illinois at Urbana-Champaign, 2015, <http://matse1.matse.illinois.edu/concrete/hist.html>

[3] A. Borosnyói, G.L. Balázs. "Models for flexural cracking in concrete: the state of the art", Structural Concrete, 6, 2005, pp. 53–62.

[4] Li, V.C., Mishra, D.K., and Wu, H.-C. "Matrix design for pseudo-strain-hardening fibre reinforced cementitious composites," Journal of Materials and Structures, Vol. 28, No. 10, Dec. 1995, pp. 586-595.

[5] Fontana, P.; Pirskawetz, S.; Lura, P.: Plastic shrinkage cracking risk of concrete - evaluation of test methods. In: Scarpas, A. et al. (eds.): Proc. 7th RILEM International conference on cracking in pavements, 20.-22.06.2012, Delft, The Netherlands, pp 591-600. ISBN: 978-94-007-4565-0.

[6] Pistol, K.; Weise, F.; Meng, B.; Diederichs, U.: Polypropylene fibres and micro cracking in fire exposed concrete. Advanced Materials Research 897 (2014), pp 284-289.

[7] Zheng, Z. and Feldman, D.: Synthetic fibre-reinforced concrete. Progress in Polymer Science 20 (1995), pp 185-210. Balaguru; P.N.; Shah, S.P.: Fiber-reinforced cement composites. USA: McGraw-Hill, Inc., 1992.

[8] Williams, E.M., Graham, S.S., Reed, P.A., and Rushing, T.S. "Laboratory Characterization of Cor-Tuf Concrete With and Without Steel Fibers," Technical Report, ERDC/GSL TR-09-22, July 2009. U.S. Army Engineer Research and Development Center, Vicksburg, MS.

[9] Roth, J.M., Rushing, T.S., Flores, O.G., Sham, D.K., and Stevens, J.W. "Laboratory Investigation of the Characterization of Cor-Tuf Flexural and Splitting Tensile Properties," Technical Report, ERDC/GSL TR-10-46, October 2010. U.S. Army Engineer Research and Development Center, Vicksburg, MS.

[10] Li, V.C. "Engineered Cementitious Composites (ECC) – Material, Structural, and Durability Performance," Chapter 24, Second Edition, Concrete Construction Engineering Handbook, 2008, CRC Press.

[11] Barnett, S.J., Lataste, J.F., Parry, T., Millard, S.G., and Soutsos, M.N. "Assessment of fibre orientation in ultra high performance fibre reinforced concrete and its effect on flexural strength," Materials and Structures, Vol. 43, 2010, pp. 1009-1023.

[12] Ferrara, L. and Meda, A. "Relationships between fibre distribution, workability and mechanical properties of SFRC applied to precast roof elements," Materials and Structures, Vol. 39, 2006, pp. 411-420.

[13] Pujadas, P., Blanco, A., Cavalaro, S., and Aguado, A. "Plastic fibres as the only reinforcement for flat suspended slabs: Experimental investigation and numerical simulation," Construction and Building Materials, Vol. 57, 2014, pp. 92-104.

[14] Woo, L.Y.; Wansom, S.; Ozyurt, N.; Mu, B.; Shah, S.P.; Mason, T.O.: Characterizing fiber dispersion in cement composites using AC-Impedance Spectroscopy. Cement and Concrete Composites 27 (2005), pp 627-636.

[15] Li, M. and Li, V.C.: Rheology, fiber dispersion, and robust properties of Engineered Cementitious Composites. Materials and Structures 46 (2013), pp 405-420.

[16] di Prisco, M., Ferrara, L., and Lamperti, M.G.L. "Double edge wedge splitting (DEWS): an indirect tension test to identify post-cracking behaviour of fibre reinforced cementitious composites," Materials and Structures, Vol. 46, 2013, pp. 1893-1918.

[17] Oesch, T.S., Landis, E.N., and Kuchma, D.A. "Conventional Concrete and UHPC Performance-Damage Relationships Identified using Computed Tomography," Journal of Engineering Mechanics, Vol. 142, No. 12, 2016.

[18] Blanco A. Characterization and modelling of SFRC elements. Doctoral Thesis. Barcelona: Universitat Politècnica de Catalunya; 2013.

[19] Morgan, I.L., Ellinger, H., Klinksiek, R., and Thompson, J.N. "Examination of concrete by computerized tomography," ACI Materials Journal, Vol. 77, 1980, pp. 23-27.

[20] Martz, H.E., Schneberk, D.J., Robertson, P.G., and Monteiro, P.J.M. "Computerized tomography analysis of reinforced concrete," ACI Materials Journal, Vol. 90, Issue 3, 1993, pp. 259-264.

[21] Bentz, D.P., Quenard, D.A., Kunzel, H.M., Baruchel, J., Peyrin, F., Martys, N.S., and Garboczi, E.J. "Microstructure and transport properties of porous building materials. II: Three- dimensional X-ray tomographic studies," Materials and Structures, Vol. 33, Issue 3, 2000, pp. 147-153.

[22] Landis, E.N., Petrell A.L., Lu, S., and Nagy, E.N. "Examination of pore structure using three dimensional image analysis of microtomographic data," Concrete Science and Engineering, Vol. 2, Issue 8, 2000, pp. 162-169.

[23] Stock, S.R., Naik, N.K., Wilkinson, A.P., and Kurtis, K.E. "X-ray microtomography (microCT) of the progression of sulfate attack of cement paste," Cement and Concrete Research, Vol. 32, No. 10, 2002, pp. 1673-1675.

[24] Oesch, T.S. "Investigation of Fiber and Cracking Behavior for Conventional and Ultra-High Performance Concretes using X-Ray Computed Tomography," Ph.D. Dissertation, 2015. University of Illinois at Urbana-Champaign, Urbana, IL.

[25] Poinard, C., Piotrowska, E., Malecot, Y., Daudeville, L., and Landis, E.N. "Compression Triaxial Behavior of Concrete: The Role of the Mesostructure by Analysis of X-Ray Tomographic Images," European Journal of Environmental and Civil Engineering, Vol. 16, Supplement 1, 2012, pp. 115-136.

[26] Bakshi, S.R., Batista, R.G., and Agarwal, A. "Quantification of carbon nanotube distribution and property correlation in nanocomposites," Composites, Part A, Vol. 40, No. 8, 2009, pp. 1311-1318.

[27] Trainor, K.J. "3-D Analysis of Energy Dissipation Mechanisms in Steel Fiber Reinforced Reactive Powder Concrete," M.S. Thesis, 2011. University of Maine, Orono, ME.
[28] Trainor, K.J., Foust, B.W, and Landis, E.N. "Measurement of Energy Dissipation Mechanisms in the Fracture of Fiber Reinforced Ultra High Strength Cement-Based Composites," Journal of Engineering Mechanics, Vol. 139, 2013, pp. 771-779.
[29] Kachanov, M., and Sevostianov, I. (2005). On quantitative characterization of microstructures and effective properties. International Journal of Solids and Structures, 42, pp. 309–336.
[30] Ferrari, M. and Johnson, G.C. Effective elasticities of short-fiber composites with arbitrary orientation distribution, Mechanics of Material, Vol. 8, 1989, pp. 67-73.
[31] Kachanov, M., Tsukrov, I., Sharo, B., 1994. Effective properties of solids with cavities of various shapes. Appl. Mech. Reviews 47 (1), 151-174.
[32] DIN EN 196-1: Methods of testing cement – Part 1: Determination of strength; May 2005
[33] Zuse Institute Berlin (ZIB): <https://amira.zib.de/>.
[34] Detlev Stalling, Malte Westerhof and Hans-Christian Hege. Amira: a Highly Interactive System for Visual Data Analysis. In: Charles D. Hansen and Chris R. Johnson (eds.), The Visualization Handbook, pp. 749-767, Elsevier, 2005.